The Journal of Experimental Biology 207, 1335-1344
Published by The Company of Biologists 2004
doi:10.1242/jeb.00869

Mitochondria-rich cell activity in the yolk-sac membrane of tilapia (*Oreochromis mossambicus*) larvae acclimatized to different ambient chloride levels

Li-Yih Lin[1] and Pung-Pung Hwang[2,*]

[1]*Graduate Institute of Life Sciences, National Defense Medical Center, Nei-Hu, Taipei 114, Taiwan, ROC* and
[2]*Institute of Zoology, Academia Sinica, Nankang, Taipei 11529, Taiwan, ROC*

*Author for correspondence (e-mail: pphwang@gate.sinica.edu.tw)

Accepted 6 January 2004

Summary

Mitochondria-rich cells (MRCs) in the yolk-sac membrane of tilapia (*Oreochromis mossambicus*) larvae were examined by Na^+/K^+-ATPase immunocytochemistry and vital staining for glycoproteins following acclimation to high (7.5–7.9 mmol l^{-1}), normal (0.48–0.52 mmol l^{-1}) or low (0.002–0.007 mmol l^{-1}) ambient Cl^- levels. With a combination of concanavalin-A (Con-A)–Texas-Red conjugate staining (larvae exposed to the dye *in vivo* in the water) and a monoclonal antibody raised against Na^+/K^+-ATPase, MRCs were easily recognized and presumed to be active when Con-A-positive (i.e. with their apical membrane in contact with the water) or inactive when Con-A-negative. The proportion of active cells gradually increased during a 48-h acclimation to low-Cl^- medium but decreased during acclimation to high-Cl^- medium. Total densities of MRCs did not change when ambient chloride levels were altered. Furthermore, in live larvae exposed to changes in ambient Cl^-, yolk-sac MRCs, vitally stained with DASPEI and subsequently traced in time, did not significantly alter turnover. The polymorphism of the apical membrane compartment of the MRCs represents structural modification of the active MRCs. Yolk-sac pavement cells labeled with the membrane marker FM1-43 (fluorescent lipophilic tracer) were shown to cover active MRCs in larvae transferred from normal to high ambient Cl^- levels, thereby inactivating the MRCs.

Key words: mitochondria-rich cell, MRC, yolk sac, tilapia, *Oreochromis mossambicus*, larva, ambient chloride.

Introduction

In embryos and larvae of several teleostean species, mitochondria-rich cells (MRCs; also called chloride cells or ionocytes) are found in the epithelia covering the yolk sac and body, and these extrabranchial MRCs are considered to be important for ion regulation during early development, when functional gills are not yet well developed (Guggino, 1980; Hwang and Sun, 1989; Ayson et al., 1994; Hwang et al., 1999; Hiroi et al., 1999).

MRC morphology and function in freshwater teleosts have previously been studied in depth, and several studies have focused on the apical membrane (often forming an apical crypt) configuration of MRCs in response to external or internal changes (Perry, 1997; Van Der Heijden et al., 1997, 1999; Marshall, 2002; Wilson and Laurent, 2002). Acidification of water increases the fractional surface area of gill MRCs without changing MRC density, indicating morphological responses of the epithelium to environment changes (Laurent and Perry, 1991), and this could result from responses of either the MRCs, a rearrangement of the pavement cells or a combination of these phenomena. Metabolic alkalosis (bicarbonate infusion) and cortisol treatment increase the number and fractional surface area of exposed MRCs in freshwater rainbow trout (*Oncorhynchus mykiss*; Perry and Goss, 1994). Laurent et al. (1995) examined the Lake Magadi tilapia (*Oreochromis alkalicus grahami*), a species uniquely adapted to severely alkaline freshwater, which possesses well-developed gill MRCs with apical crypts that remain open in alkaline water (pH 10) but close in neutral water (pH 7; within 2–3 h of exposure). Crypts appear again upon long-term (24 h) residence in neutral water, and this demonstrates the dynamics of MRC apical membrane exposure.

It is well known that the apical membrane of MRCs forms an apical crypt configuration in seawater fishes but may be flush with or raised slightly above adjacent pavement cells in most freshwater-acclimated fishes (Perry and Laurent, 1993); however, crypts have been reported for freshwater Mozambique tilapia (*Oreochromis mossambicus*) as well (Lee et al., 1996; Van der Heijden et al., 1997) and this may illustrate our limited understanding of MRC biology.

In a previous study on freshwater Mozambique tilapia, we categorized subtypes of MRCs with different apical surfaces as wavy-convex, shallow-basin and deep-hole (crypts) and correlated subtype abundance with medium Ca^{2+}, Na^+ and Cl^- concentrations (Lee et al., 1996; Chang et al., 2001). These subtypes of MRCs were suggested to be functionally different for ion transport.

More recently, we found that the morphology of these apical surfaces changed in a matter of hours with variations in ambient Cl^- concentrations and correlated with the rate of Cl^- influx in tilapia, which suggests that MRC morphology reflects distinct capabilities for Cl^- uptake (Lin and Hwang, 2001; Chang et al., 2003). In the present study, we provide further cytological evidence for the hypothesis. When ambient chloride levels are extremely reduced, gradually more active MRCs are observed and the cells enlarge their surface area, probably to upregulate their Cl^- uptake capacity; conversely, when ambient Cl^- levels are increased, MRCs are inactivated by constriction of their apical openings and become totally covered by adjacent apical pavement cells. We used immunocytochemistry and vital staining to trace the turnover of yolk-sac MRCs in tilapia larvae acclimated to high or low ambient Cl^- levels. We traced MRCs by Na^+/K^+-ATPase immunostaining and scored them as active (in contact with the water; Van der Heijden et al., 1997, 1999) when they could be labeled with Con-A–Texas-Red; we then examined the changes in active cells during chloride acclimation. In addition, yolk-sac MRCs were traced with DASPEI vital staining to examine turnover and interaction with adjacent pavement cells.

Materials and methods

Animals and various hypotonic media

Mature adult Mozambique tilapia (*Oreochromis mossambicus* L.) from the Tainan Branch of the Taiwan Fisheries Research Institute were kept in circulating freshwater at 26–28°C under a photoperiod with 12–14 h of light (Hwang et al., 1994). Tilapia eggs and larvae were available year-round from mature adults kept under controlled conditions as described above. Fertilized eggs were retrieved from the mouths of females that had initiated mouth breeding, as described previously (Hwang et al., 1994).

Three artificial freshwater media were made – (1) control, reflecting local tap water, (2) with low Cl^- content and (3) with high Cl^- content – by addition of appropriate amounts of NaCl, Na_2SO_4, $MgSO_4$, K_2HPO_4, KH_2PO_4 and $CaSO_4$ to deionized water (see Table 1). The temperature of the media was kept between 26°C and 28°C. During experiments, larvae were not fed; media were changed daily to guarantee optimal water quality.

Immunohistochemistry

Larvae were anaesthetized on ice and fixed in 4% paraformaldehyde in 0.1 mol l^{-1} phosphate buffer (PB; pH 7.4) for 30 min at 4°C. After washing with phosphate-buffered saline (PBS; pH 7.4), fixed larvae were incubated in 1 mg ml^{-1} Texas-Red-conjugated concanavalin-A (Con-A; Molecular Probes, Eugene, OR, USA; dissolved in redistilled water) for 30 min at room temperature (RT; 24–27°C). After rinsing for 20 min at 4°C, the larvae were further fixed and permeabilized with 70% ethanol at –20°C for 10 min. After washing with PBS, samples were incubated overnight at 4°C with a monoclonal antibody against the α_5-subunit of the chicken Na^+/K^+-ATPase (Developmental Studies Hybridoma Bank, University of Iowa) diluted 1:200 with PBS containing 10% normal goat serum and 1% bovine serum albumin. After rinsing with PBS for 20 min, the larvae were further incubated in goat anti-mouse IgG conjugated with fluorescein isothiocyanate (FITC; Jackson Immunoresearch Laboratories, West Grove, PA, USA; dilution 1:100) for 2 h at RT. After staining, the whole larvae were mounted in an observation chamber that was composed of a cover slip (24 mm×24 mm) and spacers slightly thinner than the thickness of the yolk sac of larvae. In this situation, the slightly compressed yolk sac provided a flatter area for observation. Observations and image acquisitions were made using a Leica TCS-NT confocal laser scanning microscope (Leica Lasertechnik, Heidelberg, Germany) equipped with 10×/0.3, 20×/0.4, 40×/1.2 and 100×/1.35 (magnification/numerical aperture) objective lenses and appropriate filter sets for simultaneous monitoring of FITC and Texas Red. Cross-talk between the two fluorescent signals was negligible in our system.

Determination of active MRCs

Two-day-old larvae were transferred from normal freshwater to the three artificial freshwater media. After 0 h (normal freshwater controls), 24 h or 48 h, larvae were sampled to determine active MRCs. MRCs were double-labeled with antibody against the sodium pump α subunit and Con-A–Texas-Red as described above. Confocal laser scanning was performed on the yolk-sac area of whole-mounts of larvae. Three areas (0.25 mm^2) per individual were scanned with a 20×/0.4 objective lens, and the acquired images were further enhanced and analyzed with MetaMorph software (Universal Imaging Corporation, Philadelphia, PA, USA). The densities of MRCs and their exposed apical surfaces were separately quantified, and the ratio of active MRCs over total MRCs was calculated as follows: active MRC (%) = (density of exposed apical surfaces/density of MRC)×100%.

Vital staining and time-sequential tracing of MRCs

Two-day-old larvae were incubated in normal freshwater containing 300 μmol l^{-1} 2-(4-dimethylaminostyryl)-1-methylpyridinium iodide (DASPEI; Sigma, St Louis, MO,

Table 1. *Ionic compositions (mmol l^{-1}) in the artificial freshwater media*

Medium	$[Na^+]$	$[Cl^-]$	$[Ca^{2+}]$	$[K^+]$	$[Mg^{2+}]$	pH
Control	0.420–0.487	0.480–0.520	0.18–0.19	0.15–0.17	0.17–0.19	6.70–6.88
Low Cl^-	10.16–10.78	0.002–0.007	0.17–0.18	0.15–0.17	0.19–0.21	6.75–6.87
High Cl^-	9.27–10.03	7.514–7.880	0.19–0.20	0.14–0.18	0.17–0.19	6.70–6.78

USA) for 2 h at 27°C. After incubation, larvae were rinsed with normal freshwater and then anesthetized with MS-222 (3-aminobenzoic acid ethyl ester; Sigma; 0.1 mg l^{-1}; pH 7.0, buffered with 3 mmol l^{-1} MOPS) for 5 min prior to observation by confocal microscopy. An individual larva was mounted in an observation chamber that was composed of a cover slip (24 mm×24 mm) and spacers (made with stacking cover slips) slightly thinner than the thickness of the yolk sac of the larvae. This chamber is similar to that used in a previous report by Hiroi et al. (1999). The flattened yolk-sac surface of the mounted larva was then analyzed by confocal laser scanning microscopy. One area (0.25 mm^2) per individual was selected for image acquisition. Usually one or more melanophores in the center of the area served as a marker to recognize the area under study during subsequent analyses. After scanning, the larvae were removed from the chamber and placed in one of several artificial freshwater tanks for further incubation. The scanning procedure was usually finished within 5 min to keep damage to the larvae to a minimum. Nine individuals from the same brood were examined in this experiment. After initial scanning, these larvae were transferred to the three media (three larvae per medium) for further incubation. After 12 h and 24 h of incubation, the same areas of the larvae were scanned again, and DASPEI-positive cells were scored. Two hours prior to the second and third scanning, DASPEI (300 μmol l^{-1}) was added to the incubation media. During the experiments, neither mortality nor significant damage occurred in the traced larvae.

Apical membrane internalization in MRCs

Live, 2-day-old larvae were immersed in a Con-A solution (1 mg Con-A–Texas-Red dissolved in 1 ml artificial water) for 30 min. Then, the larvae were transferred to Con-A-free artificial water and gently washed using a wide-mouth pipette for 3 min. After washing, the larvae were kept in artificial water, shielded from light for 2 h. Then, the larvae were sacrificed and immunolabeled for Na^+/K^+-ATPase as described above.

Simultaneous labeling of MRCs, MRC apical membranes and pavement cells

Live, 2-day-old larvae were stained with Con-A *in vivo* as described above. After washing, larvae were transferred to water with a high Cl^- content for 24 h, shielded from light to avoid photobleaching of the fluorescent probes used. After 24 h, 300 μmol l^{-1} DASPEI was added to the medium for 30 min to stain the MR cells. After washing, the larvae were transferred to an FM1-43 {*N*-(3-triethylammoniumpropyl)-4-[4-(dibutylamino)styryl]pyridinium dibromide; Molecular Probes} solution (5 μmol l^{-1}; diluted in the same medium) for 20 min to stain pavement cells.

After staining, larvae were anesthetized with MS-222 and immediately scanned with a confocal microscope. In pilots, larvae had been stained with various concentrations of FM1-43 over increasing times, which yielded similar staining intensities but increasing fluorescence intensities with concentration and time. Treatment with 5 μmol l^{-1} FM1-43 for 20 min was selected as the optimal condition for our confocal analyses.

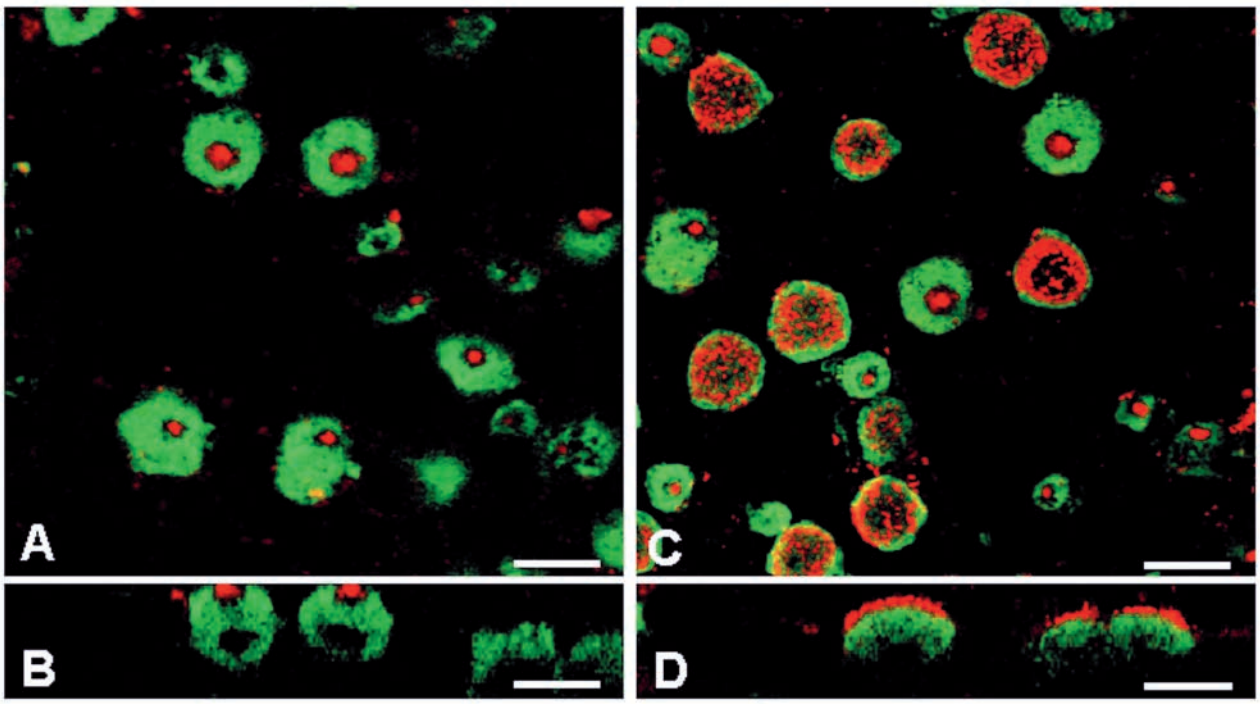

Fig. 1. Confocal scanning of yolk-sac mitochondria-rich cells (MRCs) double-labeled with Con-A–Texas-Red (red) and Na^+/K^+-ATPase antiserum (second antibody conjugated with FITC; green) in larvae acclimated to high-Cl^- medium (A,B) or low-Cl^- medium (C,D). The *x*–*y*-plane (A,C) and *z*-plane (B,D) scanning images are shown. Magnification: 1000×. Scale bars: 15 μm (A,C); 10 μm (B,D).

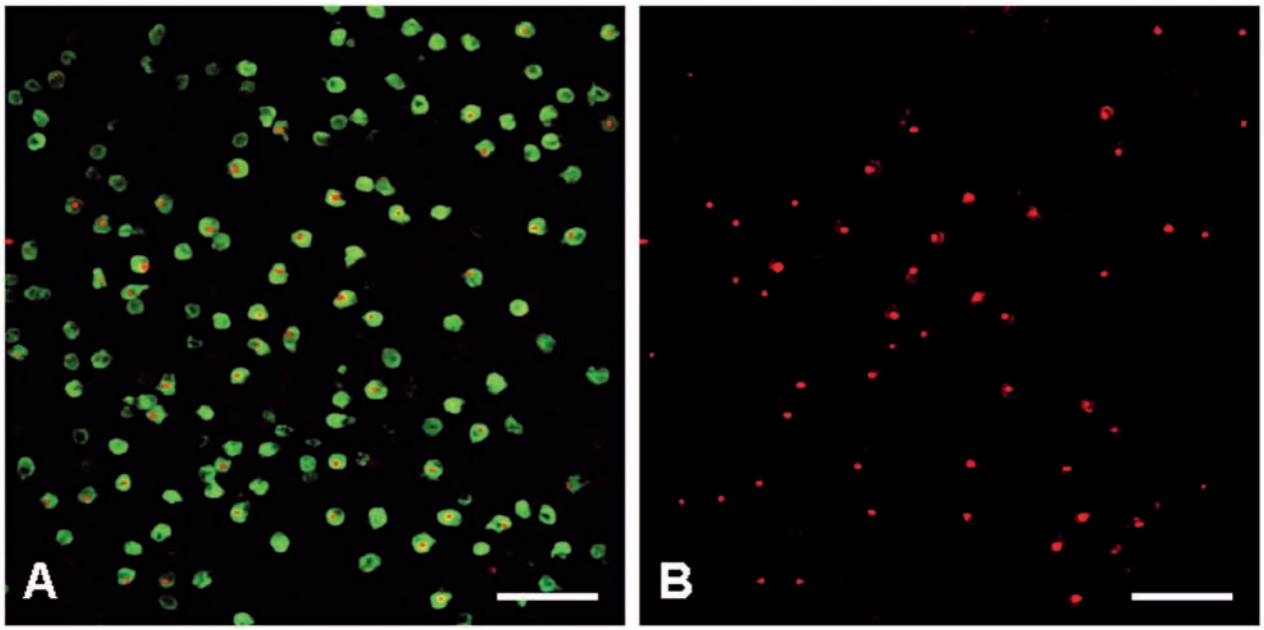

Fig. 2. Confocal scanning of yolk-sac mitochondria-rich cells (MRCs) double-labeled with Con-A–Texas-Red (red) and Na^+/K^+-ATPase antiserum (second antibody conjugated with FITC; green) in larvae. The densities of MRCs (A) and their exposed apical surfaces (B) were separately quantified, and the ratio of active MRCs over total MRCs was calculated as described in the Materials and methods. Scale bars, 50 μm.

Statistics

Values were compared using one-way analysis of variance (ANOVA) by Tukey's pair-wise method. Values are presented as means ± standard deviation (S.D.).

Results

Immunostaining and observation of MRCs

Confocal images of yolk-sac MR cells in tilapia larvae acclimatized to water with a high and low Cl^- content are shown in Fig. 1. After acclimation to these different artificial media, yolk-sac MRCs showed significant differences in Con-A labeling. In water with low Cl^- levels (Fig. 1C,D), Con-A-labeled MRCs exhibited both large, convex surfaces (~6–10 μm in diameter) and small, pinhole-like surfaces (~3–6 μm in diameter). In media with high Cl^- content, only pinhole-like MRC surfaces were observed (Fig. 1A,B). Both convex and pinhole-type MRCs were also shown in control individuals; however, the former was relatively seldom observed (data not shown). The results suggest that low Cl^- levels induce larger and convex apical surfaces in MRCs.

Active and inactive MR cells

When larvae were double-labeled with Na^+/K^+-ATPase antibody and Con-A–Texas-Red, we noticed that a portion of MRCs (rich in Na^+/K^+-ATPase labeling) were not labeled by Con-A and thus concluded that such cells are not in contact with the water (Fig. 2A). In previous studies (Lin and Hwang, 2001; Chang et al., 2003), increased density of MRCs and increased exposed surface area of the apical membrane of MRCs were shown to correlate closely and positively with Cl^-

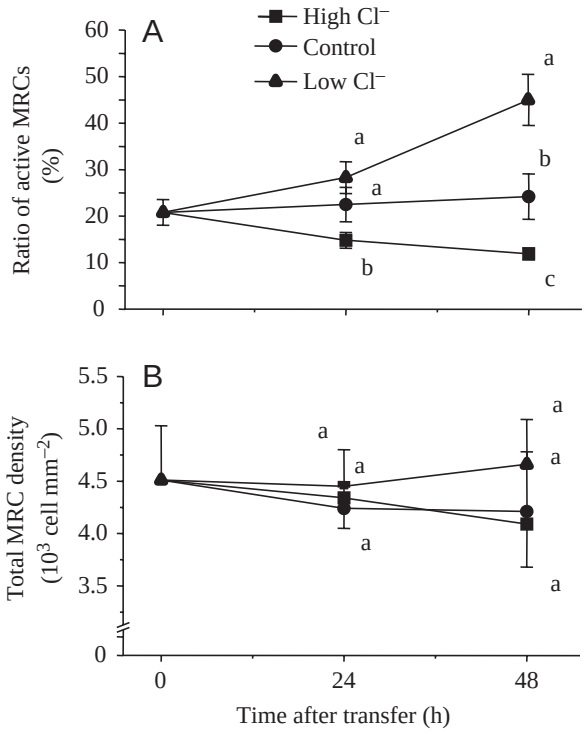

Fig. 3. Time course changes of active mitochondria-rich cells (MRCs) (A) and total MRCs (B) in yolk-sac membrane of tilapia larvae transferred from control water to low-Cl^- or high-Cl^- water for 48 h. Values are means ± S.D. (N=5). Different letters indicate significance at the P<0.05 level (one-way ANOVA followed by Tukey's pair-wise comparison).

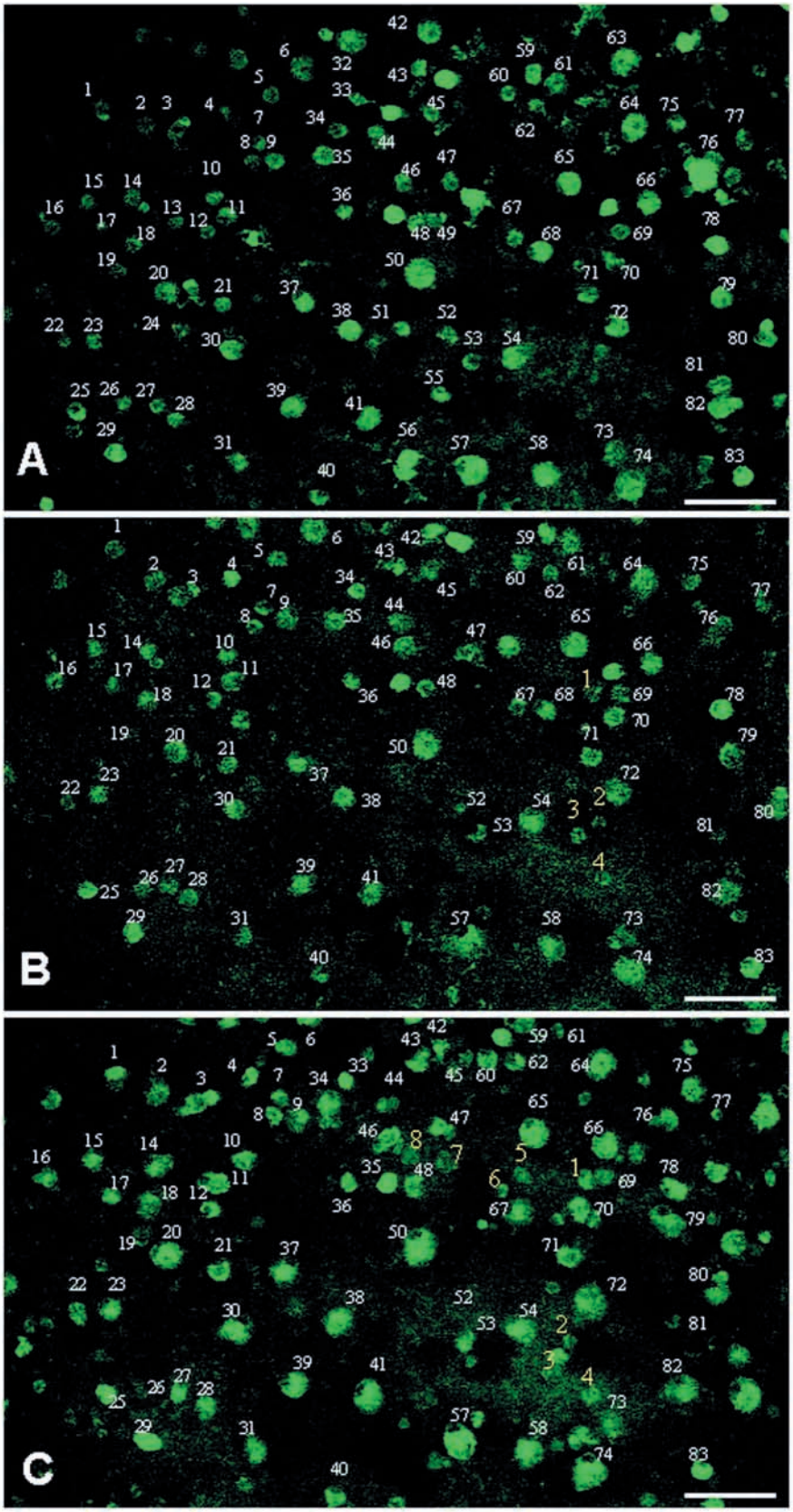

Fig. 4. Sequential observation of mitochondria-rich cells (MRCs) labeled with DASPEI in the yolk-sac membrane of tilapia larvae transferred from control to high-Cl^- water for 0 h (A; in control water), 12 h (B) and 24 h (C). White numbers mark the cells that survived the acclimation, and yellow numbers mark the new cells generated after transfer. Magnification: 200×. Scale bars: 40 μm.

influx. Based on these observations, Con-A-negative MRCs are referred to here as 'inactive' cells, in contrast to Con-A-positive, 'active' MRCs. The proportion of active MRCs of the total number of MRCs (Fig. 2) was calculated and compared between different groups of larvae acclimatized to the three media. Only ~20% of yolk-sac MRCs in 2-day-old control larvae are active, and this proportion increased slightly but significantly to 24% with development from 2 to 4 days old (Fig. 3A). However, in larvae acclimated to low Cl^- water, active MRCs increased dramatically from 20% to 45% during a 48 h acclimatization. By contrast, active MR cells declined to ~13% after 48 h in high Cl^- water (Fig. 3A). Thus, external Cl^- levels can alter the proportion of active MRCs in the yolk-sac membrane. Indeed, the density of total MRCs (active and inactive cells) in the yolk-sac membrane was similar among the three groups of larvae (Fig. 3B).

MRC dynamics

MRCs in yolk-sac membrane vitally stained with DASPEI were sequentially scanned with a confocal microscope at 12-h intervals for 24 h. During development, the yolk sacs of larvae are, of course, gradually absorbed and, during absorption, the MRCs in the yolk sac are found to a greater extent in the vicinity of the larval body trunk. However, individual MRCs keep their position relative to one another during yolk sac absorption and could be easily identified at the 12-h intervals of scanning. Fig. 4 shows confocal images of sequentially (0 h, 12 h and 24 h) scanned MRCs in larvae transferred from normal to high-Cl^- water. More than 90% of labeled cells survived the acclimation and scanning procedures (the white-numbered cells in the images; Figs 4, 5). About 10% of the cells observed over the 24 h period were new, small DASPEI-positive cells (yellow-numbered cells, Figs 4, 5). Interestingly, no significant change in DASPEI-positive cell numbers was observed in the other two groups of larvae (normal and low Cl^- water), an indication

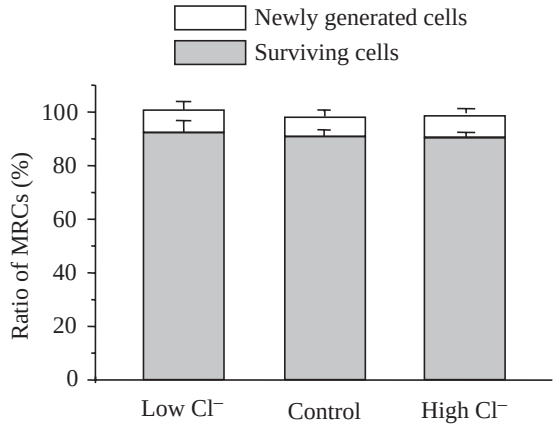

Fig. 5. Ratio of surviving or newly generated mitochondria-rich cells (MRCs) in larvae transferred from control to low-Cl^- or high-Cl^- media for 24 h. Values are means ± S.D. (*N*=3). No significant difference was found between the three groups (one-way ANOVA followed by Tukey's pair-wise comparison).

that cell turnover was not affected by a decrease in ambient Cl^- levels (Fig. 5).

Internalization of the apical membrane in MRCs

As shown by confocal optical sectioning in Fig. 6, in larvae pre-stained with Con-A and then incubated in normal water for 2 h, the Con-A-labeled apical membrane is internalized in MRCs, evidenced by punctate Con-A label (vesicles) beneath the apical membrane of MR cells (Fig. 6A). Fig. 6B,C shows optical sections 3 μm and 6 μm beneath the apical surface.

FM1-43 staining: pavement cells and apical exposure of MRCs

The lipophilic vital stain FM1-43 was used as a membrane marker to label the cell membrane of the integument epithelium. In larvae exposed to the dye in water, FM1-43 labeled mainly the integument (pavement) cells of the yolk-sac membrane, revealed as a layer of flat polygonal cells with very clearly stained cell boundaries (Fig. 7A). At high magnification (1000×), these squamous, polygonal cells showed typical characteristics of pavement cells with microridges; these cells form the outermost cell layer of the epithelium and cover the MRCs except for their apical surfaces (Fig. 7B). FM1-43 penetrates the pavement cell membrane and labels organelles inside pavement cells. When adjusting the focal plane to 3–5 μm beneath the surface of pavement cells, we observed strong signals of organelles surrounding the nuclei of pavement cells (Fig. 7C). With this staining technique, proliferating pavement cells (appearing to have 2–3 nuclei) were occasionally observed in yolk-sac membranes (Fig. 7C).

As the Con-A-labeled apical membrane of MRCs become internalized, we then set out to transfer larvae pulse-labeled with Con-A from normal water to high Cl^- water for 24 h. After this 24-h period, still-internalized Con-A vesicles were seen in MRCs, as confirmed first by DASPEI labeling. Next, larvae were stained with FM1-43 to examine the behavior of the MRCs and the pavement cells during the acclimation (Fig. 7D–F). Confocal optical sections through the surface plane (pavement cells; Fig. 7D), through a plane 6 μm beneath the surface (MRCs; Fig. 7E) and the merged picture of the two sections (Fig. 7F) showed MRCs containing Con-A-labeled vesicles (indicating that these cells had previously been in contact with the water) fully covered by pavement cells. Apparently, a high Cl^- medium forms a stimulus for active MRCs to withdraw from the surface and avoid contact with the water. In addition, the above data infer that pavement cells adjacent to MRCs fill the gaps when these cells withdraw and become inactive (no more direct contact with the ambient medium).

Discussion

In a previous study, we suggested that the three subtypes of MRCs – wavy-convex, shallow-basin and deep-hole – in yolk-sac membrane of tilapia larvae reflected MRCs possessing different capabilities, or 'activities', for Cl^- uptake (Lin and Hwang, 2001). Artificially prepared low-Cl^- water increased whole-body $^{36}Cl^-$ uptake, exposed MRC density and the proportion of the wavy-convex cells in tilapia larvae. By contrast, high-Cl^- water turned all the apical surfaces of MRCs into crypts (deep holes) and decreased their density gradually with time. By using immunocytochemistry and vital staining in the present study, we have found that the total density and even the turnover of MRCs were not altered by ambient Cl^- changes. Only the proportion of active MRCs was altered during the acclimation to different ambient Cl^- levels. Active MRCs increased in the larvae acclimated to low-Cl^- water but decreased in those acclimated to high-Cl^- water. Based on this evidence, we suggest that more active MRCs are gradually observed when ambient Cl^- levels are extremely reduced and the cells enlarge their exposed apical surfaces to upregulate Cl^- uptake activity; conversely, when ambient Cl^- levels are increased, MRCs are inactivated by constriction of their apical surfaces and gradually become totally covered by adjacent pavement cells.

We assumed that the Con-A-labeled MRCs were 'active' MRCs because they were in contact with the water through the apical surfaces, which were shown to correlate with the activity of Cl^- uptake in tilapia (Lin and Hwang, 2001; Chang et al., 2003). Conversely, MRCs completely covered by pavement cells were presumed to be 'inactive' in Cl^- uptake. In addition to the correlation between the MRC morphology and the whole-body $^{36}Cl^-$ uptake (Lin and Hwang, 2001), our recent work using a scanning ion-selective electrode technique to probe Cl^- flux in yolk-sac MRCs of tilapia has demonstrated that these unexposed MRCs are functionally inactive (L. Y. Lin and P. P. Hwang, unpublished data).

Several previous studies have employed fluorochrome-conjugated lectin to label the apical surfaces of MRCs. Li et al. (1995), Van Der Heijden et al. (1997) and Lee et al. (2000) used fluorochrome-conjugated Con-A, which binds specifically to α-glucopyranosyl glycoprotein residues, to localize the exposed

apical surfaces of MRCs identified with either mitochondrial staining or an Na^+/K^+-ATPase marker. Wheat germ agglutinin (WGA), which specifically binds to *N*-acetylglucosamine and *N*-acetylneuraminic acid residues, was also used by Tsai and Hwang (1998) to identify specific subpopulations of MRCs. Recently, Goss et al. (2001) used another lectin, peanut agglutinin (PNA; which binds specifically to terminal β-galactose residues), to separate two subtypes of MRCs. Con-A–Texas-Red has been shown to bind strongly to apical surfaces (also termed apical crypts in previous reports) of tilapia MRCs and has been used as a marker to identify exposed or mature MRCs (Li et al., 1995; Van Der Heijden et al., 1997; Lee et al., 2000). In the present study, Con-A–Texas-Red was also shown to bind specifically to apical surfaces of yolk-sac MRCs in tilapia larvae (Fig. 1). We could easily identify wavy-convex MRCs, particularly in low-Cl^- larvae. However, it was more difficult to discriminate the shallow-basin and deep-hole types due to the similar staining shape. By using Con-A–Texas-Red and Na^+/K^+-ATPase antibody double-labeling, we scored the active MRCs and examined their profiles in larvae acclimated to high- or low-Cl^- water. In normal larvae 2–4 days after hatching, 20–24% of MR cells were Con-A positive (active), which is comparable with previous data determined by counting MRCs in contact with the water environment on tissue sections of tilapia larvae (Van Der Heijden et al., 1999). The proportion of active MRCs increased from 20% to 45% after 48-h low-Cl^- acclimation but declined from 20% to 13% after high Cl^- acclimation. The changing profiles are congruent with our previous counting of exposed MRCs with scanning electronic microscopy (SEM; Lin and Hwang, 2001). However, using this double-labeling technique, we could score the active and inactive MRCs simultaneously.

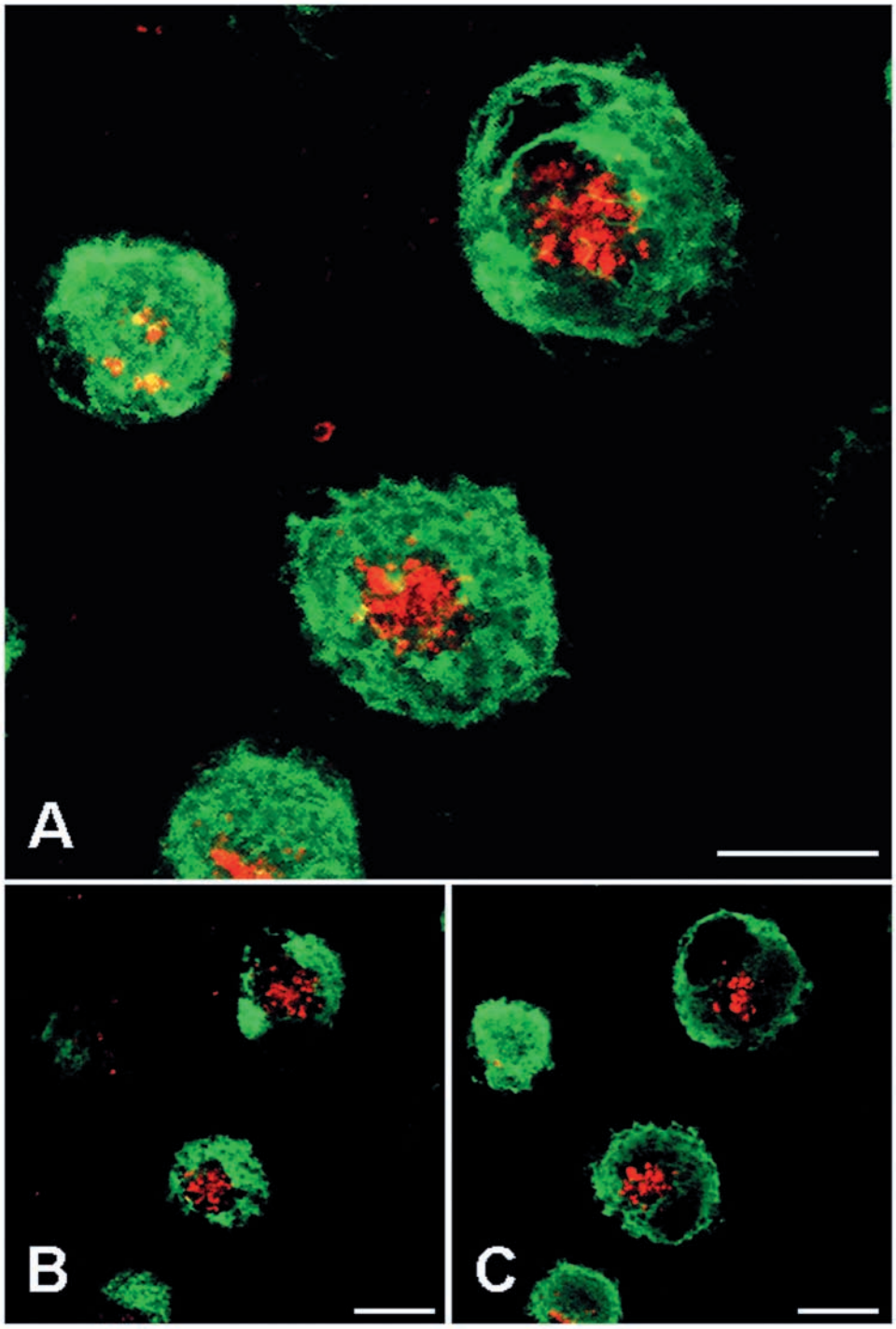

Fig. 6. Internalization of the apical membrane in mitochondria-rich cells (MRCs). Yolk-sac MRCs were double-labeled by Na^+/K^+-ATPase antiserum (second antibody conjugated with FITC; green) and Con-A–Texas-Red (red), which was internalized into the cytoplasm of MRCs (A). (B,C) Optical sections 3 μm and 6 μm beneath the apical surface. Magnification: 2000×. Scale bars: 15 μm.

In the present study, we labeled MRCs with DASPEI vital stain and sequentially monitored their turnover in intact animals during acclimation to both high- and low-Cl^- water. This method was modified from a previous report by Hiroi et al. (1999), who used it to investigate MRC turnover in tilapia larvae during seawater acclimation and found that a portion of

freshwater-type MRCs are able to transform to seawater-type MRCs. The vital stain DASPEI and its analogue DASPMI, which accumulate in active mitochondria, are the most common dyes used to label MRCs (Li et al., 1995; Witters et al., 1996; Rombough, 1999; Van Der Heijden et al., 1999). Using this technique here, we found that MRC turnover was not altered by ambient chloride changes, suggesting that the change in the densities and subtypes of MRCs induced by ambient chloride (Lin and Hwang, 2001) reflects the process of MRCs undergoing structural and functional modification.

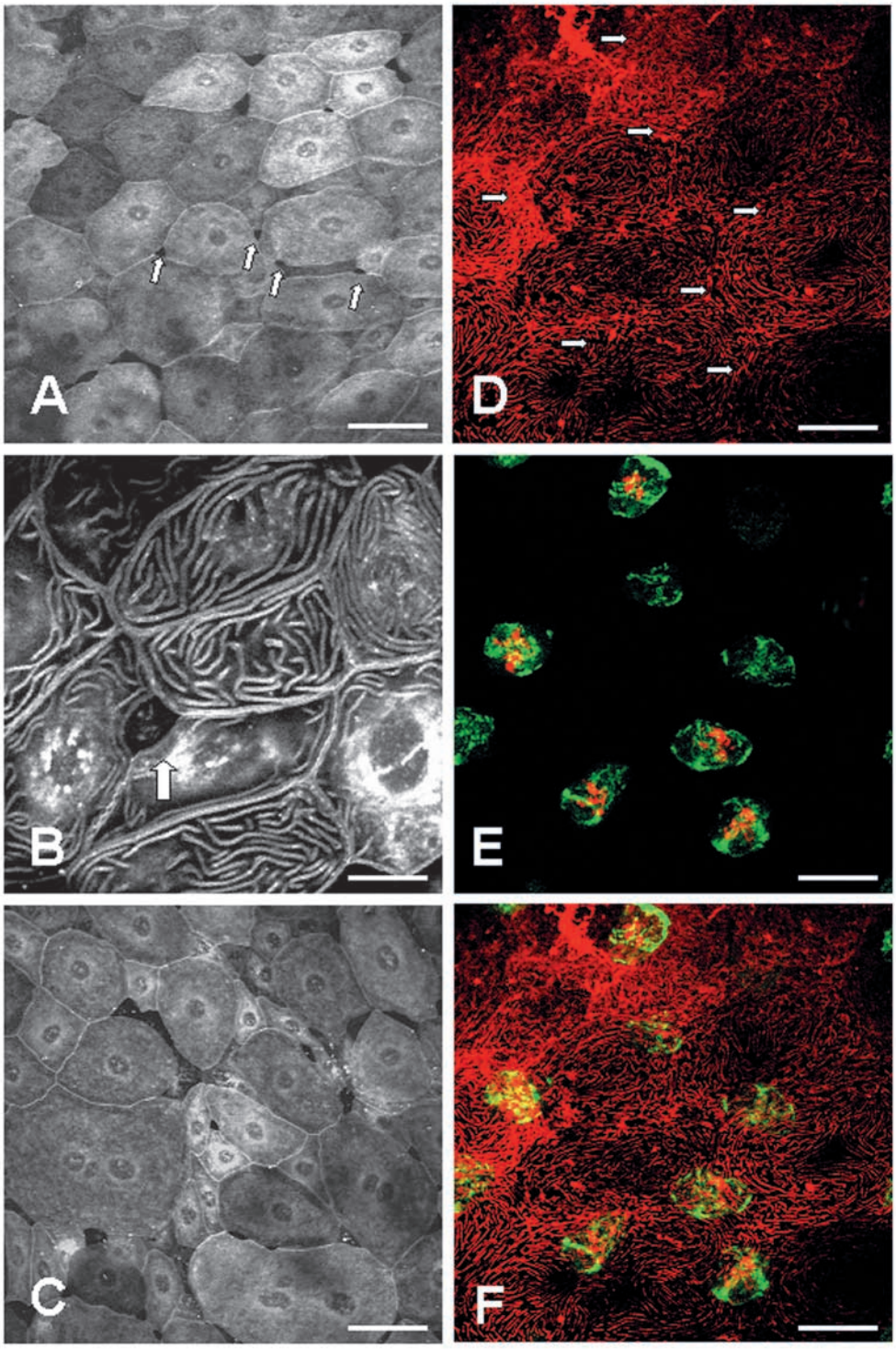

Fig. 7. FM1-43 staining and apical surface of mitochondria-rich cells (MRCs): (A–C) FM1-43 staining; (D–F) FM1-43, DASPEI and Con-A triple staining. See Results for detailed descriptions. Arrows represent the locations of MRCs. Magnification: 400× (A,C); 2000× (B); 1000× (D–F). Scale bars: 40 μm (A,C); 8 μm (B); 15 μm (D–F).

FM1-43, which was originally developed as a membrane potential sensor, has become an increasingly useful tool in the study of membrane trafficking, synaptic vesicle recycling and synaptic transmission (Cochilla et al., 1999). In addition, when used as a marker of cell membranes and surface areas, FM1-43 is useful for determining the means by which damaged cells are able to repair their membranes. Studies on endothelial cells (Miyake and McNeil, 1995), sea urchin eggs and embryos (Steinhardt et al., 1994) and crayfish medial giant axons (Eddleman et al., 1997) indicate that at the site of an injury, exocytosis of lipid vesicles is used to repair holes in the cellular membrane. In the present study, we used FM1-43 as a membrane marker to label the apical membrane of the epithelium covering the larval skin. We found that FM1-43 effectively stained the apical microstructure of pavement cells (microridges) and clearly outlined the boundary of these cells. Interestingly, we found that FM1-43 seemed to permeate the apical membrane of pavement cells and consequently stained the membrane organelles inside these cells. Since FM1-43 is used for tracing membrane trafficking (exocytosis and endocytosis), we also checked whether the vesicles inside these cells are internalized from the labeled apical membrane through endocytosis. It seems unlikely that the considerable number of vesicles is internalized from the apical membrane in such a short time (~20 min); in addition, no obvious vesicle trafficking was observed inside these cells. However, FM1-43 did not permeate MR cells but only

slightly stained their apical membranes. Applying the same method to zebrafish (*Danio rerio*) larvae, we found that FM1-43 could not penetrate the apical membrane of pavement cells, implying that the staining property is cell type and/or species dependent. A recent report found that FM1-43 also penetrates specific types of sensor neurons through mechanotransduction channels (Meyers et al., 2003). Whether or not a similar channel or conducting pathway for FM1-43 exists in tilapia pavement cells needs to be further investigated.

With FM1-43 vital staining, we could easily identify the apical surfaces of MRCs surrounded by adjacent pavement cells, similar to what we observed with SEM. However, this method allows us to investigate the morphology of pavement cells and apical surfaces of MRCs in live animals, which cannot be achieved with SEM. Using FM1-43 and DASPEI double-staining, we could simultaneously trace these two types of cells (pavement cells and MR cells) in a live animal and examine their interaction. We found that high-Cl^- water stimulated active MRCs to withdraw from the surface and avoid contact with the water. Pavement cells adjacent to MRCs play the role of filling the gaps when MRCs withdraw and become inactive.

A similar regulatory mechanism has been proposed by Goss and colleagues (Goss et al., 1992, 1998; Goss and Perry, 1993; Perry and Goss, 1994) in their studies of freshwater MRCs responding to respiratory acid–base disturbances. The present work supports their model and has adapted this regulatory mechanism to freshwater tilapia responding to ambient Cl^- disturbances. Recently, Daborn et al. (2001) used opercular membranes of killifish (*Fundulus heteroclitus*) to examine the interactions between pavement cells and MR cells during abrupt salinity changes and also concluded that osmotic shock caused MRCs to adjust their apical surface size by interacting with adjacent pavement cells. The actin cytoskeleton of MRCs was shown to maintain the apical surfaces required for modification of the surfaces in response to osmotic shock (Daborn et al., 2001). In the present study, internalization of the apical membrane of Con-A-labeled MR cells was observed, indicating that apical membrane turnover might also be involved in maintaining and regulating the structure and composition of apical surfaces. Numerous vesicles observed beneath the apical membrane of MRCs in previous reports investigating the subcellular structure of MRCs might imply the active turnover of apical membranes. The physiological significance of apical membrane turnover requires further investigation.

It has been generally accepted that MRCs that are not exposed to the external environment are undergoing differentiation and they have been considered to be functionally 'immature' MRCs (Van Der Heijden et al., 1997, 1999). However, in our findings and other reports (Laurent et al., 1995; Sakamoto et al., 2000; Daborn et al., 2001), these MRCs could be inactivated from functional cells due to being covered by pavement cells responding to ambient or internal ion/osmolarity alterations. Therefore, we use 'inactive' to describe these unexposed MRCs, which may be composed of immature and inactivated MRCs. Once upregulation of ion uptake is required, both of these forms might be recruited into becoming functionally active MR cells.

This study was supported by grants to P.-P.H. from the National Science Council (NSC 90-2313-B001-028, 91-2313-B001-033) and Academia Sinica (Major Group-Research Project), Taiwan, ROC.

References

Ayson, F. G., Kaneko, T., Hasegawa, S. and Hirano, T. (1994). Differential expression of two prolactin and growth hormone genes during early development of tilapia (*Oreochromis mossambicus*) in fresh water and seawater: implications for possible involvement in osmoregulation during early life stages. *Gen. Comp. Endocrinol.* **95**, 143-152.

Chang, I. C., Lee, T. H., Yang, C. H., Wei, Y. Y., Chou, F. I. and Hwang, P. P. (2001). Morphology and function of gill mitochondria-rich cells in fish acclimated to different environments. *Physiol. Biochem. Zool.* **74**, 111-119.

Chang, I. C., Wei, Y. Y., Chou, F. I. and Hwang, P. P. (2003). Stimulation of Cl^- uptake and morphological changes in gill mitochondria-rich cells in freshwater tilapia (*Oreochromis mossambicus*). *Physiol. Biochem. Zool.* **76**, 544-552.

Cochilla, A. J., Angleson, J. K. and Betz, W. J. (1999). Monitoring secretory membrane with FM1-43 fluorescence. *Annu. Rev. Neurosci.* **22**, 1-10.

Daborn. K., Cozzi, R. R. and Marshall, W. S. (2001). Dynamics of pavement cell–chloride cell interactions during abrupt salinity change in *Fundulus heteroclitus*. *J. Exp. Biol.* **204**, 1889-1899.

Eddleman, C. S., Ballinger, M. L., Smyers, M. E., Godell, C. M., Fishman, H. M. and Bittner, G. D. (1997). Repair of plasmalemmal lesions by vesicles. *Proc. Natl. Acad. Sci. USA* **94**, 4745-4750.

Goss, G. G., Adamia, S. and Galvez, F. (2001). Peanut lectin binds to a subpopulation of mitochondria-rich cells in the rainbow trout gill epithelium. *Am. J. Physiol. Regul. Integr. Comp. Physiol.* **281**, R1718-R1725.

Goss, G. G. and Perry, S. F. (1993). Physiological and morphological regulation of acid-base status during hypercapnia in rainbow trout (*Oncorhynchus mykiss*). *Can. J. Zool.* **71**, 1673-1680.

Goss, G. G., Perry, S. F., Wood, C. M. and Laurent, P. (1992). Mechanisms of ion and acid-base regulation at the gills of freshwater fish. *J. Exp. Zool.* **263**, 143-159.

Goss, G. G., Perry, S. F., Fryer, J. N. and Laurent, P. (1998). Gill morphology and acid-base regulation in freshwater fishes. *Comp. Biochem. Physiol. A* **119**, 107-115.

Guggino, W. B. (1980). Salt balance in embryos of *Fundulus heteroclitus* and *F. bermudae* adapted to seawater. *Am. J. Physiol.* **238**, R42-R49.

Hiroi, J., Kaneko, T. and Tanaka, M. (1999). In vivo sequential changes in chloride cell morphology in the yolk-sac membrane of Mozambique tilapia (*Oreochromis mossambicus*) embryos and larvae during seawater adaptation. *J. Exp. Biol.* **202**, 3485-3495.

Hwang, P. P., Lee, T. H., Weng, C. F., Fang, M. J. and Cho, G. Y. (1999). Presence of Na-K-ATPase in mitochondria-rich cells in the yolk-sac epithelium of larvae of the teleost *Oreochromis mossambicus*. *Physiol. Biochem. Zool.* **72**, 138-144.

Hwang, P. P. and Sun, C. M. (1989). Putative role of adenohypophysis in the osmoregulation of tilapia larvae (*Oreochromis mossambicus*; Teleostei): an ultrastructure study. *Gen. Comp. Endocrinol.* **73**, 335-341.

Hwang, P. P., Tsai, Y. N. and Tung, Y. C. (1994). Calcium balance in embryos and larvae of the freshwater-adapted teleost, *Oreochromis mossambicus*. *Fish Physiol. Biochem.* **13**, 325-333.

Laurent, P., Maina, J. N., Bergman, H. L., Narahara, A., Walsh, P. J. and Wood, C. M. (1995). Gill structure of a fish from an alkaline lake: effect of short-term exposure to neutral conditions. *Can. J. Zool.* **73**, 1170-1181.

Laurent, P. and Perry, S. F. (1991). Environmental effects on gill morphology. *Physiol. Zool.* **64**, 4-25.

Lee, T. H., Hwang, P. P., Lin, H. C. and Huang, F. L. (1996). Mitochondria-rich cells in the branchial epithelium of the teleost, *Oreochromis mossambicus*, acclimated to various hypotonic environments. *Fish Physiol. Biochem.* **15**, 513-523.

Lee, T. H., Hwang, P. P., Shieh, Y. E. and Lin, C. H. (2000). The relationship between "deep hole" mitochondria-rich cells and salinity adaptation in the euryhaline teleost *Oreochromis mossambicus*. *Fish Physiol. Biochem.* **23**, 133-140.

Li, J., Eygensteyn, J., Lock, R. A. C., Verbost, P. M., Van Der Heijden, A. J. H., Wendelaar Bonga, S. E. and Flik, G. (1995). Branchial chloride cells in larvae and juveniles of freshwater tilapia *Oreochromis mossambicus*. *J. Exp. Biol.* **198**, 2177-2184.

Lin, L. Y. and Hwang, P. P. (2001). Modification of morphology and function of integument mitochondria-rich cells in tilapia larvae (*Oreochromis mossambicus*) acclimated to ambient chloride levels. *Physiol. Biochem. Zool.* **74**, 469-476.

Marshall, W. S. (2002). Na^+, Cl^-, Ca^{2+} and Zn^{2+} transport by fish gills: retrospective review and prospective synthesis. *J. Exp. Zool.* **293**, 264-283.

Meyers, J. R., MacDonald, R. B., Duggan, A., Lenzi, D., Standaert, D. G., Corwin, J. T. and Corey, D. P. (2003). Lighting up the senses: FM1-43 loading of sensory cells through nonselective ion channels. *J. Neurosci.* **23**, 4054-4065.

Miyake, K. and McNeil, P. L. (1995). Vesicle accumulation and exocytosis at sites of plasma membrane disruption. *J. Cell Biol.* **131**, 1137-1145.

Perry, S. F. (1997). The chloride cell: structure and function in the gills of freshwater fishes. *Annu. Rev. Physiol.* **59**, 325-347.

Perry, S. F. and Goss, G. G. (1994). The effects of experimentally altered gill chloride cell surface area on acid-base regulation in rainbow trout during metabolic alkalosis. *J. Comp. Physiol. B* **164**, 327-336.

Perry, S. F. and Laurent, P. (1993). Environmental effects on fish gill structure and function. In *Fish Ecophysiology* (ed. J. C. Rankin and F. B. Jensen), pp. 231-264. London: Chapman and Hall.

Rombough, P. J. (1999). The gill of fish larvae. Is it primarily a respiratory or an ionoregulatory structure? *J. Fish Biol.* **55**, 186-204.

Sakamoto, T., Yokota, S. and Ando, M. (2000). Rapid morphological oscillation of mitochondrion-rich cell in estuarine mudskipper following salinity changes. *J. Exp. Zool.* **286**, 666-669.

Steinhardt, R. A., Bi, G. and Alderton, J. M. (1994). Cell membrane resealing by a vesicular mechanism similar to neurotransmitter release. *Science* **263**, 390-393.

Tsai, J. C. and Hwang, P. P. (1998). The wheat germ agglutinin binding sites and development of the mitochondria-rich cells in gills of tilapia (*Oreochromis mossambicus*). *Fish Physiol. Biochem.* **19**, 95-102.

Van Der Heijden, A. J. H., Van Der Meij, J. C., Flik, G. and Wendelaar Bonga, S. E. (1999). Ultrastructure and distribution dynamics of chloride cells in tilapia larvae in fresh water and seawater. *Cell Tissue Res.* **297**, 119-130.

Van Der Heijden, A. J. H., Verbost, P. M., Eygensteyn, J., Li, J., Wendelaar Bonga, S. E. and Flik, G. (1997). Mitochondria-rich cells in gills of tilapia (*Oreochromis mossambicus*) adapted to fresh water or seawater: quantification by confocal laser scanning microscopy. *J. Exp. Biol.* **200**, 55-64.

Wilson, J. M. and Laurent, P. (2002). Fish gill morphology: inside out. *J. Exp. Zool.* **293**, 192-213.

Witters, H., Berckmans, P. and Vangenechten, C. (1996). Immunolocalization of Na^+, K^+-ATPase in the gill epithelium of rainbow trout, *Oncorhynchus mykiss*. *Cell Tissue Res.* **283**, 461-468.